Published in final edited form as:

J Neurosci Res. 2014 February ; 92(2): 195–205. doi:10.1002/jnr.23320.

Oxidative Damage and Amyloid-β Metabolism in Brain Regions of the Longest-Lived Rodents

Yael H. Edrey[1,2], **Salvatore Oddo**[1,2], **Carolin Cornelius**[3], **Antonella Caccamo**[1], **Vittorio Calabrese**[3], and **Rochelle Buffenstein**[1,2,*]

[1]Department of Physiology, University of Texas Health Science Center at San Antonio, San Antonio, Texas

[2]The Barshop Institute for Aging and Longevity Studies, University of Texas Health Science Center at San Antonio, San Antonio, Texas

[3]Department of Chemistry, Faculty of Medicine, University of Catania, Catania, Italy

Abstract

Naked mole rats (NMRs) are the longest-lived rodents, with young individuals having high levels of Aβ in their brains. The purpose of this study was twofold: to assess the distribution of Aβ in key regions of NMR brains (cortex, hippocampus, cerebellum) and to understand whether the accumulation of Aβ is due to enhanced production or decreased degradation. Recent evidence indicates that lipid peroxides directly participate in induction of cytoprotective proteins, such as heat shock proteins (Hsps), which play a central role in the cellular mechanisms of stress tolerance. Amyloid precursor protein processing, lipid peroxidation, Hsps, redox status, and protein degradation processes were therefore assessed in key NMR brain regions. NMR brains had high levels of lipid peroxidation compared with mice, and the NMR hippocampus had the highest levels of the most toxic moiety of Aβ (soluble $A\beta_{1–42}$). This was due not to increased Aβ production but rather to low antioxidant potential, which was associated with low induction of Hsp70 and heme oxygenase-1 as well as low ubiquitin-proteasome activity. NMRs may therefore serve as natural models for understanding the relationship between oxidative stress and Aβ levels and its effects on the brain.

Keywords

naked mole rats; Alzheimer's disease; autophagy; ubiquitin-proteasome pathway; insulin degrading enzyme; isoprostanes; heat shock proteins

Oxidative damage to terminally differentiated neurons is regarded as a leading cause of Alzheimer's disease (AD; Bonda et al., 2010). AD is characterized by the progressive loss of synapses and/or neurons and worsening deficits to cognitive function. Oxidative stress may exacerbate accumulation of oxidative damage by downregulating antioxidants and

*Correspondence to: Rochelle Buffenstein, Barshop Institute for Longevity and Aging Studies, University of Texas Health Science Center at San Antonio, 15355 Lambda Drive, STCBM No. 2.2, San Antonio, TX 78209. buffenstein@uthscsa.edu.

degradation processes. In AD, these altered functions all contribute to the accumulation of Aβ (for review see Bonda et al., 2010; Riederer et al., 2011).

A decline in hippocampal volume is considered a reliable predictor for mild and moderate dementia. Oxidative damage in the hippocampus is evident in the preclinical (PCAD) stages of AD (Lovell et al., 2011). Indeed, the hippocampus is commonly regarded as the initiation site of neuronal loss or damage in AD, spreading to the cortex and eventually affecting the entire brain (Gosche et al., 2002). In contrast, the cerebellum appears relatively impervious to these forms of insults until the late stages of the disease (Rapoport et al., 2000). It is not known whether the human hippocampus is more protected against oxidative damage or more pro-oxidative and/or has poorer antioxidant defenses than other regions, thus contributing to its increased vulnerability. Nevertheless, antioxidants are routinely proposed as a therapeutic approach to combat the pathological changes in AD (Joseph et al., 2003; Pocernich et al., 2011).

Amyloid-β (Aβ) is formed from a sequential cleavage of amyloid precursor protein (APP), a ubiquitous membrane protein thought to be involved in synapse formation and neural plasticity (Priller et al., 2006). Accumulation of Aβ can be caused by overproduction as a result of increased activity of the β- and γ-secretases, such as in the familial form of AD (for review see Gotz et al., 2011), or by impairments to mechanisms for its removal, as was recently shown in a human study (Mawuenyega et al., 2010). Aβ degradation is orchestrated by various mechanisms including insulin-degrading enzyme (IDE), autophagy, and the ubiquitin-proteasome pathway (UPS; Kurochkin and Goto, 1994; Oddo, 2008; Caccamo et al., 2010). Manipulating these levels in AD mouse models resulted in a correlation with Aβ levels in either direction, depending on the modification (Farris et al., 2003; Miller et al., 2003; Leissring et al., 2003; Spilman et al., 2010; Majumder et al., 2011; Medina et al., 2011).

Long-lived naked mole rats (*Heterocephalus glaber*; NMRs), show high levels of oxidative damage to visceral tissues even at a young age (Andziak and Buffenstein, 2006; Andziak et al., 2006). Surprisingly, this does not appear to affect their aging negatively. NMRs are not only able to live an additional 20 years with these high levels of oxidative damage but also show delayed and attenuated age-related declines in physiological function, molecular markers, and behavior for at least 75% of their 32-year maximal life span (Buffenstein, 2008). Surprisingly, Aβ levels were found to be high in young (2–9 years) NMR brain, and similar to those shown in 3xTg-AD mice (Edrey et al., 2013). Nevertheless, these young NMRs have the potential to live an additional ~20–30 years in captivity and maintain seemingly normal cognitive functions.

NMRs are eusocial subterranean mammals and live in large colonies. They rely on spatial orientation to navigate through a maze of underground burrows and exhibit complex social interactions and conspecific communication. In humans (and other mammals), many of these functions are known to be regulated by the hippocampus, a brain region considered the epicenter of AD. The unexpected observation of high levels of Aβ in young NMRs led us to ask two questions: 1) Are these levels dispersed evenly across the brain? 2) are these high levels the result of increased production of Aβ or lower efficiency in degradation? We

hypothesized that, in young NMRs, the hippocampus would be spared from high levels of Aβ because of either low production or increased degradation. We therefore compared Aβ metabolism in cortex, hippocampus, and cerebellum of young NMRs and investigated a possible relationship among Aβ distribution, levels of heat shock proteins (Hsps), and redox status in these brain regions.

MATERIALS AND METHODS

Animals

Young, nonbreeding NMRs were specifically chosen for this study rather than aged individuals. In nongenetically manipulated animal populations there is considerable natural variation in any trait, and this variation is generally much greater in the elderly population. Young animals enable us to observe intraindividual variation in Aβ levels, production and degradation in specific brain regions without confounding variables from increasing age. Animals are maintained in colonies and are monitored and cleaned daily. Ambient temperature is maintained at 28–30°C with a relative humidity of 40% to mimic conditions found in NMR underground burrows and kept in the dark except during feeding/cleaning. NMRs have been maintained in our captive colony for over 3 decades, and all animals used in this study were born in captivity. Animal procurement and euthanasia were carried out in adherence to NIH, Federal, State, and Institutional guidelines and were approved by the IACUC committee at UTHSCSA (protocol 07123). Tissues were harvested from young (4–6 months) C57Bl/6 mice and (1–2 year) nonbreeding NMRs of both sexes. These are considered physiologically age matched, because the proportion of life lived in each species is similar to encompass early adulthood. In some instances, whole brains (minus cerebellum and brainstem) were used for interspecies comparisons; otherwise, brain regions were dissected on ice to separate cerebellum, hippocampus, and cortex. All samples were flash frozen in liquid nitrogen and stored in −80°C until use.

Statistical Analysis

SigmaPlot v.11 (San Jose, CA) was used for statistical analysis. *t*-Tests were used for comparisons between two groups. Analysis of variance (ANOVA) was used when there were three or more groups, with Holm-Sidak for post hoc analysis, unless otherwise stated. Significance was determined at $P = 0.05$.

Lipid Peroxidation

Levels of isoprostanes (F_2-IsoPs) were used as an indicator of oxidative stress. Five whole-brain samples from each species (not including cerebellum and brainstem) were used for inter-species comparisons. Because the various brain regions were too small for individualized measurements, samples from two same-sex littermates were pooled, and six different samples for 12 individuals for the cortices, hippocampi, and cerebella were analyzed. F_2-IsoPs were determined using a stable isotope dilution method with detection by gas chromatography/negative-ion chemical ionization/mass spectrometry (GC-NICI-MS) as previously described (Ward et al., 2005). Briefly, 100–200 mg tissue was homogenized in ice-cold Folch solution (chloroform/methanol 2:1) containing 5 mg/100 ml butylatedhydroxytoluene (BHT). Lipids were then extracted and chemically hydrolyzed with

15% KOH. After acidification with HCl, a stable isotope, 8-*iso*-prostaglandin $F_{2\alpha}$-d_4, internal standard was added. After extraction using C-18 and silica Sep-Pac cartridges, the eluted compounds were dried under N_2, then converted to pentafluororobenzyl esters and purified by thin-layer chromatography (TLC). The purified F_2-isoprostanes were derivatized to trimethysilyl ether derivatives, then dissolved in undecane for quantification by GC/MS. Negative ion chemical ionization MS was performed with Agilent 6890 GC and Model 5975 MSD instruments with selected ions monitored for [$^2H_4$]15-$F_{2\alpha}$-IsoP internal standard (m/z 573) and F_2-IsoPs (m/z 569).

Antioxidants

A colorimetric copper-reducing assay (Total Antioxidant Power; Oxford Biomedical Research) was performed. Five samples per region were homogenized in ice-cold phosphate-buffered saline (PBS), pH 7.0, and centrifuged at 3,000*g* for 12 min at 4°C. Samples were assessed in duplicate, and the experiment was performed per manufacturer's instructions. Absorbance was measured at 450 nm using a spectrophotometer (Molecular Devices, Sunnyvale, CA), and averages were calculated. Data are mean ± SEM. Levels of cytoplasmic superoxide dismutase 1 (SOD1) were assessed by immunoblot with the antibody to SOD1 (1:2,000; goat; R&D Systems, Minneapolis, MN; AF3787). These were analyzed in ImageJ (NIH), and data are mean ± SEM.

Glutathione (Reduced and Oxidized) Assay

Four samples per brain region were used for GSH/GSSG measurements using a modified protocol based on the methods described by Adams et al. (1983) to adjust for a microplate reader. For GSH, a standard curve was produced ranging from 5 to 50 nmoles/ml for GSH (Sigma, St. Louis, MO; G4251) and 0.1–10 nmoles/ml for GSSG (Sigma; 150568). The various brain regions were homogenized in 500 μl solution containing 10 mM DTNB in 100 mM potassium phosphate, pH 7.5, which contained 17.5 mM EDTA, and 100 μl of this solution was added to 0.5 U glutathione reductase from baker's yeast (G3664; Sigma) in 100 mM potassium phosphate and 5 mM EDTA, pH 7.5 (buffer 1). The reaction was initiated with 220 nmol NADPH in buffer 1 for a final reaction volume of 250 μl per well, and the change in absorbance over 10 min was read at 412 nm with a spectrophotometer (Molecular Devices). For GSSG, 300 μl homogenate was added to 300 &mghr;l 10 mM NEM (Sigma) in 100 mM potassium phosphate and 17.5 mM EDTA, pH 6.5 (buffer 2); mixed; and centrifuged at 2,000*g* for 6 min. The supernatant was added to Sep-Pak C18 cartridges (Waters, Dublin, Ireland) that had been pretreated with methanol and ddH_2O. The cartridge was then washed with 600 μl ddH_2O. Aliquots of the eluted solution were randomly assigned to microplate wells containing 250 nmol DTNB and 0.5 U glutathione reductase and initiated with NADPH as with the GSH samples for a total volume of 250 μl per well, and absorbance was read at 412 nm. All samples were processed in duplicates in tandem with the appropriate standard curves. An aliquot of the original samples was used to measure protein content (Pierce, Rockford, IL), and final measurements were normalized by protein content.

Quantification of Soluble and Insoluble Aβ

Four NMR samples per brain region were homogenized in T-PER buffer (Pierce) containing protease (Roche Complete Mini) and phosphatase inhibitors (Calbiochem, La Jolla, CA; 1:100) for the soluble fractions. Aβ levels were measured as per Oddo et al. (2005). Briefly, samples were centrifuged at 100,000*g* for 1 hr at 4°C, and the supernatant was collected for the soluble fraction portion. Insoluble fractions were produced by reconstitution of the resulting pellet in 70% formic acid and centrifugation at 100,000*g* for 1 hr at 4°C. To attain standard curves, serial dilutions of synthetic $A\beta_{40}$ and $A\beta_{42}$ were made ranging from 39 to 20,000 pg/ml per plate. Samples and standards were run in duplicate on the same plate. Wells were pre-treated with $A\beta_{1–16}$ 20.1 antibody (1:20) for 2 days at 4°C and blocked (3% bovine sreum albumin) for 3 hr at 37°C, and thereafter soluble fractions were directly applied to 96-well plates, and insoluble fractions were diluted in neutralization buffer (1 M Tris base 0.5 M NaH_2PO dibasic, 1:20). Wells were washed with PBS and treated with antigen capturing buffer (20 mM NaH_2PO4, 2 mM EDTA, 0.4 M NaCl, 0.5 g CHAPS, 1% BSA, pH 7.0). Wells were washed and treated with horseradish peroxidase-conjugated anti-$A\beta_{35–40}$ antibody C49 for $A\beta_{40}$ (1:1,000) or anti-Aβ35–42 D32 antibody for $A\beta_{42}$ (1:500) overnight at 4°C and labeled with streptavidin for 4 hr before treatment with 3,3′,5,5′-tetramethylbenzidine as a chromogen and read at 450 nm in a spectrophotometer (Molecular Devices). Values were normalized by protein content (BCA). Eight-month-old 3xTg-AD mice were used as positive controls for all fractions.

Immunoblots

NMR samples were sonicated on ice in buffer containing 0.01% Triton and protease inhibitors and centrifuged at 20,000*g* for 20 min. Ten percent NuPage Bis-Tris gels were transferred to nitrocellulose membranes and were treated with antibodies for APP and C-terminal fragments (1:1,000; rabbit; Calbiochem; 171610). NuPage Midi gels (4–12%) were transferred to PVDF membranes and treated with IDE antibody (1:1,000; rabbit; Abcam, Cambridge, United Kingdom; ab32216). The epitope (EFKRGLPLFPLVKPH) of this antibody is 100% homologous between NMRs (Genbank accession EHb13111.1) and mouse (accession AAH41675.1), so direct interspecies comparisons could be made. During autophagy, the cytoplasmic form of the microtubule-associated protein light chain 3 (LC3) is recruited to the autophagosome, thereby generating LC3II. The ratio of LC3II to LC3I is therefore used as a marker for autophagy by immunoblotting to LC3 (1:1,000; rabbit; Cell Signaling, Beverly, MA; 2775) using 16.5% Bis-Tris gels (Criterion) transferred to PVDF membranes. When probed for Hsp70 or heme-oxygenase 1 (HO-1), membranes were incubated with anti-Hsp72 antibody (1:1,000; monoclonal; Amersham, Arlington Heights, IL; RPN 1197) that recognizes only the inducible form, or, respectively, with anti-HO-1 antibodies (1:1,000; Stressgen, Vancouver, British Columbia, Canada). For detection of inducible Hsp70, the membranes were incubated with a horseradish peroxidase-conjugated sheep anti-mouse immunoglobulin G (IgG), followed by enhanced chemiluminescence (ECL; Amersham). Blots probed for HO-1 were visualized using an amplified alkaline phosphatase kit from Sigma (Extra 3A). The amounts of Hsp70 and HO-1 were quantified by scanning Western blot-imaged films with a laser densitometer (LKB-Ultroscan, XL model). All blots were normalized for actin (Calbiochem; JA20). Data were analyzed in ImageJ (NIH) and are mean ± SEM.

UPS

Eight samples per species were used for whole-brain comparisons, and five samples per species were used for the brain region comparisons of total proteolytic and proteasome activity. Chymotrypsin-like activity (CT-L) was measured with or without inhibition by MG132 (Calbiochem) and is therefore represented as total and net (inhibited) activity. The net activity represents the specific proteasome peptidolytic activity (Rodriguez et al., 2010). Tissue was homogenized in PBS, pH 7.0, and centrifuged for 12 min at 3,000*g*, 4°C, and supernatants were assessed for protein content (Pierce). Twenty-five or fifty micrograms protein was added to 100 μM of the fluorogenic substrate SucLLVY-AMC (Boston Biochem, Boston, MA; S-280), which is specific for CT-L activity. Upon proteolytic activity, AMC is released and fluorescence recorded. Samples of whole brains or brain regions were randomly assigned to a 96-well fluorescence plate in duplicate, and measurements were taken every minute for a total of 60 min at 37°C using a spectrophotometer (Molecular Devices). The slope per reaction was calculated, averaged per sample, and compared with a standard curve with known amounts of AMC (0.5–10 mM). Net activity was calculated by subtracting the inhibited values from the total values and represents proteasome (net) activity (Rodriguez et al., 2010) compared with total (noninhibited) proteolytic activity.

RESULTS

Oxidative Stress and Damage

In keeping with previous findings of high oxidative damage in the viscera of NMR tissues (Andziak et al., 2006), brains of young NMRs had significantly (*t*-test $P = 0.013$) higher levels of F_2-IsoPs (Fig. 1A) compared with physiologically age-matched young mice. Regional samples from young NMR brains, however, were not significantly different (Fig. 1B; $F = 1.712$, $P = 0.219$), suggesting that in NMRs no one region is better protected than another from oxidative stress.

Antioxidant Activity

The “Total Antioxidant Power” assay reflects activity from enzymatic antioxidants as well as large and small molecules that act as neutralizing agents to counter oxidative stress. In NMRs, average levels of total antioxidant capacity were not significantly different among brain regions (Fig. 1C; $P = 0.078$). Average SOD1 expression levels (Fig. 1D) were also similar in the three brain regions ($P = 0.083$). These data suggest that the NMR hippocampus does not have a better antioxidant defense than other brain regions.

The antioxidant GSH appears in three different ways, 1) as the amount of total GSH, 2) as oxidized GSSG, and 3) as GSH/GSSG. GSH (Fig. 2A) was similar in all NMR brain regions ($P = 0.430$). Similarly, the oxidized form GSSG (Fig. 2B) did not differ among the three brain regions ($P = 0.346$) and GSH/GSSG (Fig. 2C) did not differ between these brain regions ($P = 0.683$). In mice, GSH did not differ between these regions, but GSSG was higher in cerebellum compared with hippocampus and cortex. GSH/GSSG was lowest in the cerebellum of mice (Calabrese et al., 2002).

Aβ Accumulation

Detectable levels of Aβ were evident in all three NMR brain regions (Fig. 3). These levels were comparable to those found in 3xTg-AD mouse whole-brain homogenates. Levels of soluble $A\beta_{1–40}$ did not significantly differ in NMR brain regions (Fig. 3A; F = 2.642, P = 0.125). The soluble $A\beta_{1–42}$ fraction showed a high variance in hippocampal samples, significantly higher than that in the cortex (Fig. 3B; ANOVA on ranks, Tukey $P < 0.05$). Levels of insoluble $A\beta_{1–40}$ and $A\beta_{1–42}$ were similar among the three NMR brain regions (Fig. 3C, F = 0.658, P = 0.541 and Fig. 3D, F = 0.238, P = 0.793), respectively.

Aβ Production

Levels of full-length APP did not differ among NMR brain regions (Fig. 4A; P = 0.836). However, APP processing appeared to be reduced in the hippocampus: C83, a footprint of α-secretase cleavage, was lowest in hippocampus (Fig. 4B; F = 20.03, P = 0.001). Similarly, C99, the remainder after β-secretase cleavage, was also lowest in the hippocampus (Fig. 4C; F = 5.873, P = 0.027). These findings suggest that, although the levels of full-length APP are not altered within regions, the processing of this protein by both α- and β-secretase is reduced in hippocampus.

Degradation Processes

Young, healthy, wild-type mice naturally show low levels of Aβ and were therefore used as a “baseline” control with which to assess rates of Aβ degradation. Expression levels of IDE, a protein known to promote Aβ degradation, did not change among brain regions of either species (Fig. 5A; P = 0.164, P = 0.101, respectively). Moreover, IDE levels in both mice and NMRs were similar (P = 0.164), suggesting that this mode of Aβ degradation is not a key player in the species differences in Aβ observed. Both species have identical epitopes to the IDE antibody (see Materials and Methods).

Lower values of autophagy, measured by LC3II/LC3I immunoblotting ratios, were observed in NMR brain homogenates compared with wild-type mice. This may reflect species differences in antibody recognition or that autophagy in the NMR brain is lower than in mice. To avoid this potential problem with interspecific comparisons, LC3II/LC3I ratios from each brain region were normalized to the cortex values for their corresponding species. LC3II/LC3I ratios were not different among the various brain regions in mice (Fig. 5C; gray; P = 0.105), suggesting that autophagy is similar in these regions. However, in NMRs, the cerebellum stood out in having significantly lower levels of autophagy than the cortex and hippocampus (Fig. 5C; white; F = 10.414, P = 0.011).

Protein degradation by UPS activity was significantly higher in the homogenates of the NMR brain relative to the mouse brain. Total CT-L activity was threefold higher in NMR brain homogenates than in mice (Fig. 6A; P = 0.004). This species difference was even greater when CT-L net activity was measured by treating the lysates with a proteasome-specific inhibitor (MG132) and thereby removing the contribution of non-specific proteases (Fig. 6B; $P < 0.001$). Inhibition induced by MG132 in whole-brain tissue lysates was similar in the two species (P = 0.29). In mice, this inhibition differed among regions, with significantly higher inhibition in cortex (81.3% ± 1.3) compared with cerebellum (67.02%

± 1.4) and hippocampus (65.4% ± 2.4; F = 27.9, $P < 0.001$). These findings may indicate a greater presence of nonspecific proteases in the latter two regions. In NMRs, the same dose of MG132 resulted in no significant differences in inhibition among regions (72.5% ± 8.2%; $P = 0.383$).

Total CT-L activity (Fig. 6C) and proteasome-specific CT-L activity (Fig. 6D) (i.e., net) CT-L activity showed a different pattern in each species. In mice, activity (Fig. 6D) was highest in hippocampus, followed by cortex and cerebellum (F = 39.96, $P < 0.001$; F = 36.3, $P < 0.001$; respectively). In contrast, NMR net CT-L activity was similar among all three regions ($P = 0.169$). Thus, levels of Aβ degradation are not significantly enhanced in the hippocampus of the NMR.

Hsps

The average basal levels of inducible Hsp70 (Fig. 7A) were significantly different among the NMR brain regions (F = 94.7, $P < 0.001$). Cerebella showed the highest amounts compared with both the cortex ($P < 0.001$) and the hippocampus ($P = 0.020$). Similarly, the average HO-1 (Fig. 7C) was significantly different between the NMR brain regions (F = 52.32, $P < 0.001$), with the highest concentration in the cerebellum compared with hippocampus ($P < 0.001$) and cortex ($P < 0.001$).

DISCUSSION

Given the important role that communication, navigation skills, and memory play in NMR life, we hypothesized that the hippocampus would be protected from Aβ accumulation and that this would be due to lower production or higher degradation of Aβ. Our findings do not support this hypothesis. Certain characteristics of the young NMR hippocampus suggest that it may be significantly more susceptible to the harmful effects of Aβ and oxidatively induced damage than the other brain regions examined. It is difficult to incorporate a direct interspecies analysis because of confounding factors such as core temperature, social structure, maximum life span, and other variables, between the NMR and mouse. Therefore, we used an intraspecies comparison between three key brain regions of the NMR to test our hypothesis.

Life in hyperoxic atmospheres relative to those found in their natural hypoxic underground habitat may explain the higher levels of oxidative damage in NMR brains compared with physiologically age-matched mice (Fig. 1A). No particular brain region stood out as having the highest levels of lipid peroxidation (Fig. 1B), nor glutathione (Fig. 2C). Collectively, these data do not suggest that the hippocampus is better protected than other brain regions.

Surprisingly, young NMR brains contain high levels of Aβ (Edrey et al., 2013). By comparing three brain regions from the same young animals, we were able to test our hypothesis that the hippocampus would have low Aβ levels. Brain regions of young NMRs had high levels of all forms of Aβ, with levels similar to those observed in 3xTg-AD mice. In NMRs, levels of the soluble forms of Aβ were higher than those of the insoluble forms. This is not surprising; the soluble forms are precursors to the insoluble forms, and the data set included only young animals. Current AD research suggests that the soluble form is more

harmful than the insoluble form and that $A\beta_{1–42}$ is more toxic than $A\beta_{1–40}$ (for review see LaFerla et al., 2007). It therefore appears that the NMR hippocampus has the highest levels of the most harmful moiety-soluble $A\beta_{1–42}$ (Fig. 3B).

The NMR APP cleavage products C83 and C99 were lowest in the hippocampus, suggesting that both α-and β-secretase activities were lower in this region compared with cortex and cerebellum. Why this should be the case, given the similar levels of APP in the other brain regions, is not known. One hypothesis revolves around the negative feedback loop associated with APP processing. Hippocampal neural activity modulates APP processing, whereas the accumulation of Aβ in turn may cause synaptic depression (Kamenetz et al., 2003), leading to cognitive deficits. Although these measurements were made in young NMR brains, which ought to be functioning at their prime, it is plausible that the already high levels of Aβ in the hippocampus are leading to lower neural activity and the resultant decline in APP processing. Nevertheless, given the low levels of the amyloidogenic fragment of APP (C99), the high levels of Aβ present in the hippocampus cannot be attributed to enhanced Aβ production in this region (Fig. 4). Rather, mechanisms that degrade and clear Aβ could be responsible for the divergent Aβ levels in the brain regions.

IDE is a metalloprotease enzyme (Kurochkin and Goto, 1994) with lower expression and activity in the hippocampus of AD brains (Cook et al., 2003). NMRs and mice show similar patterns of IDE levels, with no significant differences among the regions under examination within or between each species (Fig. 5A). Therefore, it is unlikely that IDE plays a role in regional differences in Aβ levels. Similar levels among mice and NMRs were unexpected; IDE is thought not only to regulate insulin degradation but to be regulated itself by insulin levels (Zhao et al., 2004). Pronounced interspecies differences between NMRs and mice in insulin levels and handling have been reported (for review see Edrey et al., 2011).

In healthy mammals, autophagy and UPS degrade Aβ (Mawuenyega et al., 2010; for review see Jaeger and Wyss-Coray, 2010), whereas impairments to these processes are implicated in the progression of AD (Nixon et al., 2005; Pickford et al., 2008; Oddo et al., 22008; Medina et al., 2011). Importantly, increasing autophagy or UPS in AD-mouse models lowers Aβ loads, with concomitant cognitive rescue (Spilman et al., 2010; Majumder et al., 2011; Medina et al., 2011). It was therefore hypothesized that regional differences in autophagy or UPS-mediated removal of oxidatively damaged proteins may account for the high levels of Aβ in the NMR hippocampus. The marker for autophagy, LC3-II/LC3-I, did not significantly differ among the brain regions of mice (Fig. 5C). In NMRs, the cerebellum had significantly lower levels compared with either hippocampus or cortex. Unlike young rats and mice (Zeng et al., 2005), NMRs did not exhibit regional differences in CT-L activity (Fig. 6). Data from wild-type mice used in the present study support those previously published (Zeng et al., 2005) and show higher levels of CT-L activity in the cortex than in the cerebellum. Interestingly, we report that the highest levels observed in mice were in the hippocampus (Fig. 6C,D). Enhanced UPS-mediated degradation, in contrast, was not observed in the NMR hippocampus. Rather, both total proteolytic CT-L activity and proteasome-specific cleavage (net activity) tended to be lowest in this region, indicating that it is less able to clear Aβ load compared with the cortex and cerebellum. Consistently with this, we found lower levels of expression in Hsp70 and HO-1 in the hippocampus compared

with the cerebellum (Fig. 7). To prevent cellular damage on proteasome inhibition, there is an upregulation of several heat shock proteins (Hsps), including vitagenes Hsp70 and HO-1 (Calabrese et al., 2011), which are involved in the heat shock response and the KEAP1/NRF2/ARE pathways. For the latter, evidence exists that its component HO-1 can be a prooxidant, both directly and through the indirect mechanism of CO-mediated vasodilation; however, together with the heat shock system these responses provide the cell with carefully orchestrated, broad defense mechanisms with versatile cytoprotective functions. Moreover, deficiencies in these systems are associated with accelerated pathogenesis of many chronic degenerative diseases and aging (Cornelius et al., 2013). NMRs show high levels of Nrf2 in both visceral tissues (Lewis et al., 2010) and cells in culture (Lewis et al., 2012) compared with mice, although, surprisingly, no significant differences were found among the NMR brain regions (data not shown). It is therefore likely that regional differences in both Hsp70 expression and UPS-mediated degradation contribute to the observed elevated levels of Aβ in the NMR hippocampus. The interplay between autophagy and UPS activity is not entirely understood, but perhaps autophagy is higher in NMR hippocampus as a compensatory process for lower UPS activity in this region resulting from oxidative stress and reduced antioxidant activity.

In human AD patients, UPS function in hippocampus is impaired both structurally and functionally, and this is attributed to the high levels of oxidative stress (e.g., lipid peroxidation; Keller et al., 2000). Given the high levels of soluble $A\beta_{1–42}$ in NMR hippocampus, it is possible that the observed lower UPS activity is linked to high levels of oxidative damage evident in the NMR brain. Compared with other regions in the brain, in response to learning and other novel events, the hippocampus is constantly undergoing structural reorganization and modification of neuronal circuits and retains structural plasticity throughout life (Leuner and Gould, 2010). The hippocampus of NMRs shows a remarkable ability to cope with stress such as oxygen and nutrient deprivation (Larson and Park, 2009; Nathaniel et al., 2009, 2013). Although this structural plasticity may be essential for learning and memory, it is possible that a tradeoff exists between the maintenance of hippocampal plasticity and protection against oxidative stress and Aβ accrual. If the same holds true in human brains, this may explain in part why the hippocampus is the first brain region to be affected in AD.

To summarize, our hypothesis that the NMR hippocampus would have low levels of Aβ was refuted. Rather, this region has the highest levels of the most toxic form of Aβ, soluble $A\beta_{1–42}$. This was not due to higher levels of APP or Aβ production or to degradation mechanisms associated with IDE or autophagy but rather was linked to lower levels of UPS-mediated Aβ degradation associated with low Hsp levels. Higher levels of Aβ accrual in the brain region responsible for learning and creating new memories may reflect the need to maintain hippocampal structural plasticity in order to continue to learn and respond to new environmental challenges. However, this may be at the expense of protecting this vital region from Aβ accrual. Moreover, if this is indeed the case, it may explain why the hippocampus is the first region to develop signs of AD pathology in humans. These data further suggest that, given the exceptionally long life span of this species, NMRs may indeed be vulnerable to the development of sporadic AD.

Acknowledgments

Contract grant sponsor: NIA/NIH, Contract grant number: AG022891 (to R.B.); Contract grant sponsor: Glenn Foundation (to R.B.).

References

Adams JJ, Lauterburg B, et al. Plasma glutathione and glutathione disulfide in the rat: regulation and response to oxidative stress. J Pharmacol Exp Ther. 1983; 227:749–754. [PubMed: 6655568]

Andziak B, Buffenstein R. Disparate patterns of age-related changes in lipid peroxidation in long-lived naked mole-rats and shorter-lived mice. Aging Cell. 2006; 5:525–532. [PubMed: 17129214]

Andziak B, O'Connor T, et al. High oxidative damage levels in the longest-living rodent, the naked mole-rat. Aging Cell. 2006; 5:463–471. [PubMed: 17054663]

Baruch-Suchodolsky R, Fischer B. Abeta40, either soluble or aggregated, is a remarkably potent antioxidant in cell-free oxidative systems. Biochemistry. 2009; 48:4354–4370. [PubMed: 19320465]

Benzi G, Pastoris O, et al. Influence of aging and drug treatment on the cerebral glutathione system. Neurobiol Aging. 1988; 9:371–375. [PubMed: 3141824]

Bonda D, Wang X, et al. Oxidative stress in Alzheimer disease: a possibility for prevention. Neuropharmacology. 2010; 59:290–294. [PubMed: 20394761]

Bradley MA, Markesbery WR, et al. Increase levels of 4-hydroxynonenal and acrolein in the brain in preclinical Alzheimer's disease (PCAD). Free Radic Biol Med. 2010; 48:1570–1576. [PubMed: 20171275]

Buffenstein R. Negligible senescence in the longest living rodent, the naked mole-rat: insights from a successfully aging species. J Comp Physiol B Biochem Syst Environ Physiol. 2008; 178:439–445.

Caccamo A, Majumder S, et al. Molecular interplay between mammalian target of rapamycin (mTOR), amyloid-beta, and Tau: effects on cognitive impairments. J Biol Chem. 2010; 285:13107–13120. [PubMed: 20178983]

Calabrese V, Scapagnini G, et al. Regional distribution of heme oxygenase, HSP70, and glutathione in brain: relevance for endogenous oxidant/antioxidant balance and stress tolerance. J Neurosci Res. 2002; 68:65–75. [PubMed: 11933050]

Calabrese V, Cornelius C, et al. Hormesis, cellular stress response and vitagenes as critical determinants in aging and longevity. Mol Aspects Med. 2011; 32:279–304. [PubMed: 22020114]

Chang K, Suh Y. Possible roles of amyloid intracellular domain of amyloid precursor protein. BMB Rep. 2010; 43:656–663. [PubMed: 21034527]

Cook D, Leverenz J, et al. Reduced hippocampal insulin-degrading enzyme in late-onset Alzheimer's disease is associated with the apolipoprotein E-epsilon4 allele. Am J Pathol. 2003; 162:313–319. [PubMed: 12507914]

Cornelius C, Perrotta R, et al. Stress responses, vitagenes and hormesis as critical determinants in aging and longevity: mitochondria as a chi. Immun Ageing. 2013; 10:15. [PubMed: 23618527]

Edrey YH, Park T, et al. Endocrine function and neurobiology of the longest-living rodent, the naked mole-rat. Exp Gerontol. 2011; 46:116–123. [PubMed: 20888895]

Edrey YH, Medina DX, et al. Amyloid beta and the longest-lived rodent; the naked mole-rat as a model for natural protection from Alzheimer's disease. Neurobiol Aging. 2013

Farris W, Mansourian S, et al. Insulin-degrading enzyme regulates the levels of insulin, amyloid beta-protein, and the beta-amyloid precursor protein intracellular domain in vivo. Proc Natl Acad Sci USA. 2003; 100:4162–4167. [PubMed: 12634421]

Gosche K, Mortimer J, et al. Hippocampal volume as an index of Alzheimer neuropathology: findings from the Nun Study. Neurology. 2002; 58:1476–1482. [PubMed: 12034782]

Gotz J, Eckert A, et al. Modes of Abeta toxicity in Alzheimer's disease. Cell Mol Life Sci. 2011; 68:3359–3375. [PubMed: 21706148]

Hyder F, Patel A, et al. Neuronal–glial glucose oxidation and glutamatergic–GABAergic function. J Cereb Blood Flow Metab. 2006; 26:865–877. [PubMed: 16407855]

Jacobsen K, Iverfeldt K. Amyloid precursor protein and its homologues: a family of proteolysis-dependent receptors. Cell Mol Life Sci. 2009; 66:2299–2318. [PubMed: 19333550]

Jaeger P, Wyss-Coray T. Beclin 1 complex in autophagy and Alzheimer disease. Arch Neurol. 2010; 67:1181–1184. [PubMed: 20937944]

Jolivet R, Magistretti P, et al. Deciphering neuron–glia compartmentalization in cortical energy metabolism. Front Neuroenerget. 2009; 1:4.

Joseph J, Denisova N, et al. Blueberry supplementation enhances signaling and prevents behavioral deficits in an Alzheimer disease model. Nutr Neurosci. 2003; 6:153–162. [PubMed: 12793519]

Kamenetz F, Tomita T, et al. APP processing and synaptic function. Neuron. 2003; 37:925–937. [PubMed: 12670422]

Kapogiannis D, Mattson M. Disrupted energy metabolism and neuronal circuit dysfunction in cognitive impairment and Alzheimer's disease. Lancet Neurol. 2011; 10:187–198. [PubMed: 21147038]

Keller J, Hanni K, et al. Possible involvement of proteasome inhibition in aging: implications for oxidative stress. Mech Ageing Dev. 2000; 113:61–70. [PubMed: 10708250]

Kurochkin I, Goto S. Alzheimer's beta-amyloid peptide specifically interacts with and is degraded by insulin degrading enzyme. FEBS Lett. 1994; 345:33–37. [PubMed: 8194595]

LaFerla F, Green K, et al. Intracellular amyloid-beta in Alzheimer's disease. Nat Rev Neurosci. 2007; 8:499–509. [PubMed: 17551515]

Larson J, Park TJ. Extreme hypoxia tolerance of naked mole-rat brain. Neuroreport. 2009; 20:1634–1637. [PubMed: 19907351]

Leissring M, Farris W, et al. Enhanced proteolysis of beta-amyloid in APP transgenic mice prevents plaque formation, secondary pathology, and premature death. Neuron. 2003; 40:1087–1093. [PubMed: 14687544]

Leuner B, Gould E. Structural plasticity and hippocampal function. Annu Rev Psychol. 2010; 61:111–140. C111–C113. [PubMed: 19575621]

Lovell M, Soman S, et al. Oxidatively modified nucleic acids in preclinical Alzheimer's disease (PCAD) brain. Mech Ageing Dev. 2011; 132:443–448. [PubMed: 21878349]

Lewis KN, Mele J, et al. Nrf2, a guardian of healthspan and gatekeeper of species longevity. Integr Comp Biol. 2010; 50:829–843. [PubMed: 21031035]

Lewis KN, Mele J, et al. Stress resistance in the naked mole-rat: the bare essentials—a mini review. Gerontology. 2012; 58:453–462. [PubMed: 22572398]

Ma H, Lesne S, et al. Involvement of beta-site APP cleaving enzyme 1 (BACE1) in amyloid precursor protein-mediated enhancement of memory and activity-dependent synaptic plasticity. Proc Natl Acad Sci USA. 2007; 104:8167–8172. [PubMed: 17470798]

Majumder S, Richardson A, et al. Inducing autophagy by rapamycin before, but not after, the formation of plaques and tangles ameliorates cognitive deficits. PloS One. 2011; 6:e25416. [PubMed: 21980451]

Mawuenyega K, Sigurdson W, et al. Decreased clearance of CNS beta-amyloid in Alzheimer's disease. Science. 2010; 330:1774. [PubMed: 21148344]

Medina D, Caccamo A, et al. Methylene blue reduces abeta levels and rescues early cognitive deficit by increasing proteasome activity. Brain Pathol. 2011; 21:140–149. [PubMed: 20731659]

Miller B, Eckman E, et al. Amyloid-beta peptide levels in brain are inversely correlated with insulysin activity levels in vivo. Proc Natl Acad Sci USA. 2003; 100:6221–6226. [PubMed: 12732730]

Morimoto R, Cuervo A. Protein homeostasis and aging: taking care of proteins from the cradle to the grave. J Gerontol Ser A Biol Med Sci. 2009; 64:167–170.

Nathaniel TI, Saras A, et al. Tolerance to oxygen nutrient deprivation in the hippocampal slices of the naked mole rats. J Integr Neurosci. 2009; 8:123–136. [PubMed: 19618484]

Nathaniel TI, Otukonyong EE, et al. Metabolic regulatory clues from the naked mole rat: toward brain regulatory functions during stroke. Brain Res Bull. 2013; 98C:44–52. [PubMed: 23886571]

Nixon R, Wegiel J, et al. Extensive involvement of autophagy in Alzheimer disease: an immuno-electron microscopy study. J Neuropathol Exp Neurol. 2005; 64:113–122. [PubMed: 15751225]

Oddo S. The ubiquitin-proteasome system in Alzheimer's disease. J Cell Mol Med. 2008; 12:363–373. [PubMed: 18266959]

Oddo S, Caccamo A, et al. Triple-transgenic model of Alzheimer's disease with plaques and tangles: intracellular Abeta and synaptic dysfunction. Neuron. 2003; 39:409–421. [PubMed: 12895417]

Oddo S, Caccamo A, et al. Chronic nicotine administration exacerbates tau pathology in a transgenic model of Alzheimer's disease. Proc Natl Acad Sci USA. 2005; 102:3046–3051. [PubMed: 15705720]

Pickford F, Masliah E, et al. The autophagy-related protein beclin 1 shows reduced expression in early Alzheimer disease and regulates amyloid beta accumulation in mice. J Clin Invest. 2008; 118:2190–2199. [PubMed: 18497889]

Pocernich C, Lange M, et al. Nutritional approaches to modulate oxidative stress in Alzheimer's disease. Curr Alzheimer Res. 2011; 8:452–469. [PubMed: 21605052]

Priller C, Bauer T, et al. Synapse formation and function is modulated by the amyloid precursor protein. J Neurosci. 2006; 26:7212–7221. [PubMed: 16822978]

Qiu W, Folstein M. Insulin, insulin-degrading enzyme and amyloid-beta peptide in Alzheimer's disease: review and hypothesis. Neurobiol Aging. 2006; 27:190–198. [PubMed: 16399206]

Rapoport M, van Reekum R, et al. The role of the cerebellum in cognition and behavior: a selective review. J Neuropsychiatry Clin Neurosci. 2000; 12:193–198. [PubMed: 11001597]

Riederer B, Leuba G, et al. The role of the ubiquitin proteasome system in Alzheimer's disease. Exp Biol Med. 2011; 236:268–276.

Rodriguez K, Gaczynska M, et al. Molecular mechanisms of proteasome plasticity in aging. Mech Ageing Dev. 2010; 131:144–155. [PubMed: 20080121]

Sapolsky R. Glucocorticoids and hippocampal atrophy in neuro-psychiatric disorders. Arch Gen Psychiatry. 2000; 57:925–935. [PubMed: 11015810]

Spilman P, Podlutskaya N, et al. Inhibition of mTOR by rapamycin abolishes cognitive deficits and reduces amyloid-beta levels in a mouse model of Alzheimer's disease. PloS One. 2010; 5:e9979. [PubMed: 20376313]

Ward W, Qi W, et al. Effects of age and caloric restriction on lipid peroxidation: measurement of oxidative stress by F2-isoprostane levels. J Gerontol Ser A Biol Med Sci. 2005; 60:847–851.

Zeng B, Medhurst A, et al. Proteasomal activity in brain differs between species and brain regions and changes with age. Mech Ageing Dev. 2005; 126:760–766. [PubMed: 15888331]

Zhao W, Chen H, et al. Insulin and the insulin receptor in experimental models of learning and memory. Eur J Pharmacol. 2004; 490:71–81. [PubMed: 15094074]

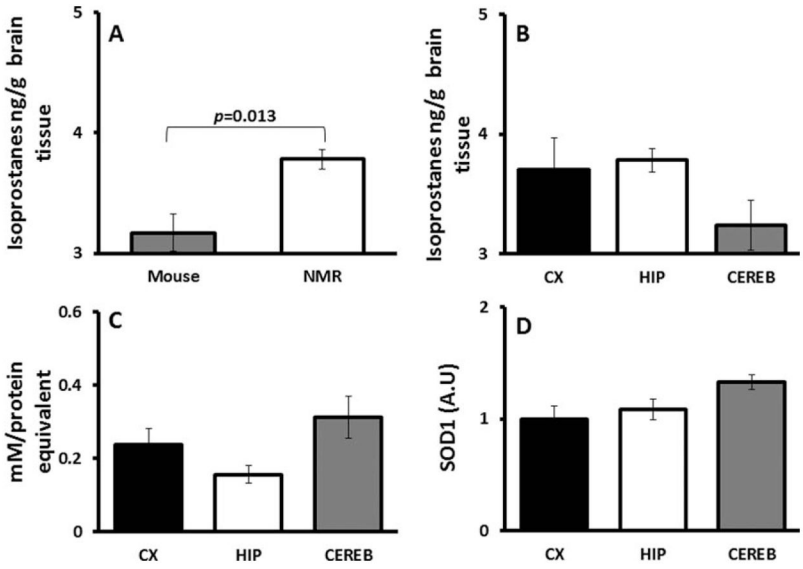

Fig. 1.

Lipid peroxidation and antioxidants in NMR brains. **A:** Physiologically age-matched young NMRs (2 years; 3.784 ± 0.152 ng/g tissue) had 1.2-fold higher levels of isoprostanes (*t*-test $P = 0.013$) in brain tissue than young mice (4–6 months; 3.168 ± 0.082 ng/g tissue; n = 5). **B:** Samples from young NMR brain regions show no significant differences (ANOVA F = 2.789, $P = 0.121$) among cortex (3.945 ± 0.322 ng/g tissue), hippocampus (3.846 ± 0.108 ng/g tissue), and cerebellum (3.258 ± 0.139 ng/g tissue). **C:** Total antioxidant capacity was not significantly different among cerebellum (0.312 ± 0.06 mM protein equivalent), cortex (0.236 ± 0.04), and hippocampus (0.155 ± 0.02; ANOVA $P = 0.078$). Data are mean ± SEM (n = 5). **D:** Expression levels of SOD1 show the highest activity in cerebellum (1.32 ± 0.06), with similar levels in cortex (1.0 ± 0.11) and hippocampus (1.08 ± 0.09), although this is not significant (ANOVA $P = 0.083$). Data are SEM and are relative to expression levels in cortex (n = 4).

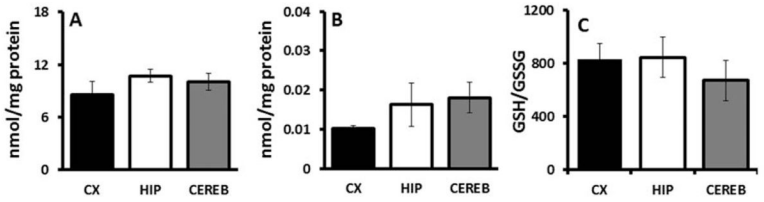

Fig. 2.

Glutathione and redox index among brain regions of NMRs. **A:** GSH as a measure of total glutathione is not significantly different among cortex, hippocampus, or cerebellum (ANOVA, F = 0.929, $P = 0.430$). **B:** The oxidized form GSSG does not differ among these brain regions (ANOVA, F = 1.216, $P = 0.346$). **C:** GSH/GSSG also does not differ among these brain regions (ANOVA, F = 0.398, $P = 0.683$). Data are mean ± SEM (n = 4).

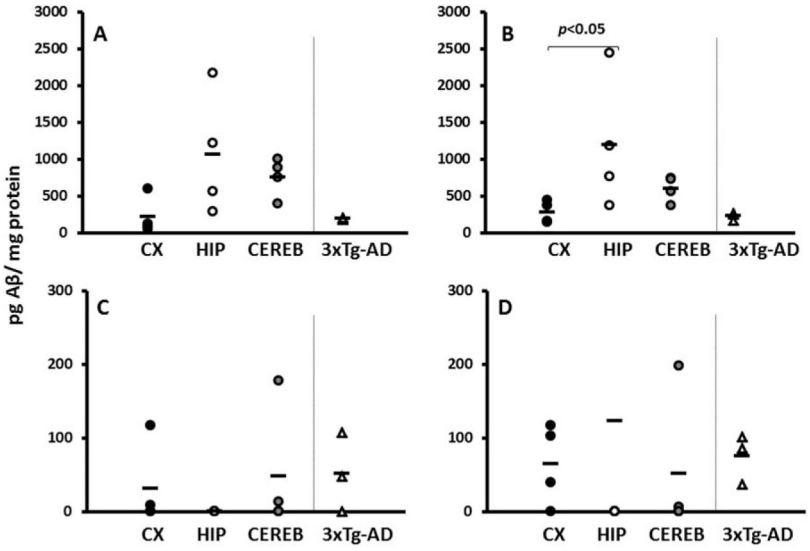

Fig. 3.

Aβ levels in young NMRs are comparable to those of young 3xTg-AD mice. ELISA results reveal that young NMRs have detectable levels of Aβ in cortex (black circles), hippocampus (white circles), and cerebellum (gray circles). **A:** Levels of soluble $A\beta_{1–40}$ do not significantly differ in NMR brain regions (ANOVA, $P = 0.125$). **B:** Levels of soluble $A\beta_{1–42}$ are significantly higher in hippocampus compared with cortex (ANOVA on ranks, Tukey $P < 0.05$). **C:** Levels of insoluble (formalin-extractable) $A\beta_{1–40}$ do not differ significantly among the three brain regions (ANOVA $P = 0.541$). **D:** Levels of insoluble (formalin-extractable) $A\beta_{1–42}$ also do not significantly differ among the three brain regions (ANOVA $P = 0.793$). In all cases, NMR levels are comparable to those of young (8 month) 3xTg-AD mice (triangles). Units are picograms Aβ per milligram protein (n = 4 for NMRs, n = 3 for mice).

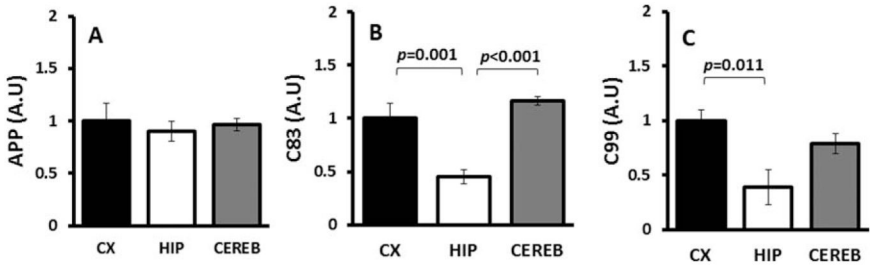

Fig. 4.

Regional differences in Aβ production. **A:** Full-length APP as measured by immunoblot is similar among all regions (ANOVA F = 0.185, $P = 0.836$). **B:** C83, the product of APP after α-secretase cleavage of APP, is reduced in the hippocampus (ANOVA F = 20.0, $P = 0.001$). **C:** C99, the terminal fragment that remains after β-secretase cleavage, is also lowest in the hippocampus of young NMRs (ANOVA F = 5.873, $P = 0.027$). Data from immunoblots were normalized to cortex and are mean ± SEM (n = 4).

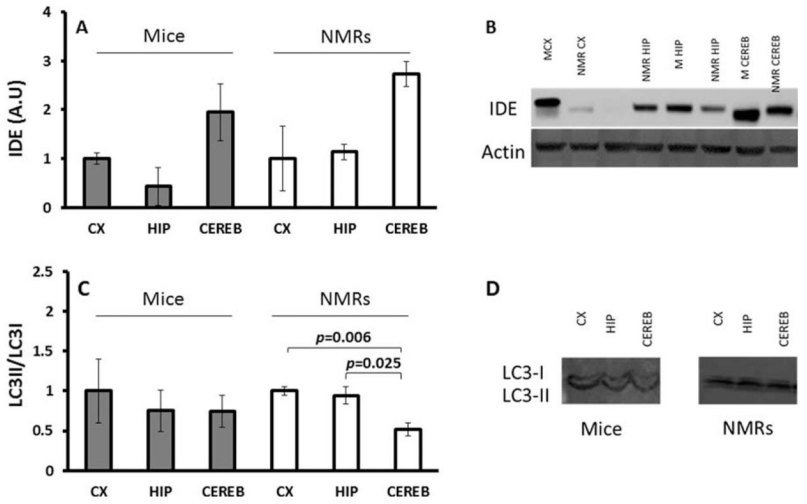

Fig. 5.

Degradation in young mice and NMRs. **A:** Expression levels of IDE as measured by immunoblot are not significantly different among brain regions of young mice (ANOVA F = 3.505, $P = 0.164$; in gray) or NMRs (ANOVA F = 5.398, $P = 0.101$; in white). **B:** Representative image of immunoblot stained for IDE. **C:** Ratio of LC3II/LCI as a measure of autophagy does not significantly change with brain regions in mice (ANOVA F = 0.902, $P = 0.105$). In NMRs, levels in cerebellum are lowest (ANOVA F = 10.414, $P = 0.011$) compared with both cortex ($P = 0.006$) and hippocampus ($P = 0.025$). **D:** Representative image of immunoblot stained for LC-3. Data for both sets of immunoblots were normalized to cortex per each species and are mean ± SEM (n = 4).

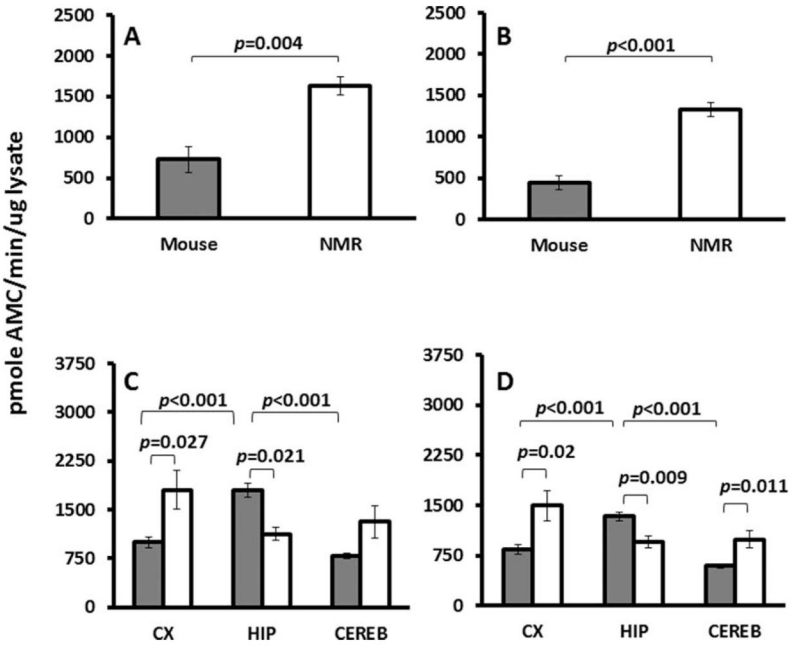

Fig. 6.

Chymotrypsin-like activity is species and region dependent. **A:** Total chymotrypsin-like activity is 2.23-fold higher in NMR brains (1,630.71 ± 157.4) than in mice brains (729.93 ± 113.9; *t*-test $t = -4.636$, DF = 6, $P = 0.004$) as measured by kinetic UPS assay. **B:** Net activity (total activity inhibited by MG132) is threefold higher in NMR brains (1,326.51 ± 87.41) than in mice brains (442.67 ± 89.77; *t*-test $t = -7.054$, DF = 6, $P < 0.001$). Inhibition with MG132 revealed a significant difference (*t*-test $t = -7.086$, DF = 6, $P < 0.001$) between NMRs and mice (81.5% and 62.4%, respectively). Data are mean ± SEM (n = 5). **C:** Total CT-L activity in mice was highest in hippocampus (1,798.5 ± 114.0), followed by cortex (997.2 ± 8.83) and cerebellum (788.7 ± 34.3; ANOVA F = 39.96, $P < 0.001$). In NMRs, similar activity levels were evident among cortex (1,804.8 ± 300.2), cerebellum (1,314.7 ± 249.9), and hippocampus (1,128.1 ± 95.7; ANOVA $P = 0.169$). **D:** Net activity reveals a similar pattern for CT-L activity, suggesting that most of the activity originates from the proteasome. Mice had the highest levels in hippocampus (1,333.5 ± 67.0), followed by cortex (842.2 ± 78.2) and cerebellum (593.2 ± 25.9). In NMRs, levels were similar in cortex (1,495.3 ± 224.4), cerebellum (990.7 ± 124.8), and hippocampus (955.6 ± 86.8; ANOVA $P = 0.060$). Activity was inhibited with MG132 to produce the net activity, and average levels for both species were not significantly different (*t*-test $P = 0.29$). In mice, inhibition was highest in cortex (81.3 ± 1.3), followed by cerebellum (67.02 ± 1.4) and hippocampus (65.4 ± 2.4; ANOVA DF = 2, F = 27.9, $P < 0.001$). In NMRs, inhibition was similar in the three regions: cortex (80.9% ± 2.7), hippocampus (81.7% ± 1.3) and cerebllum (72.5% ± 7.7; ANOVA $P = 0.383$). Data are mean ± SEM (n = 8).

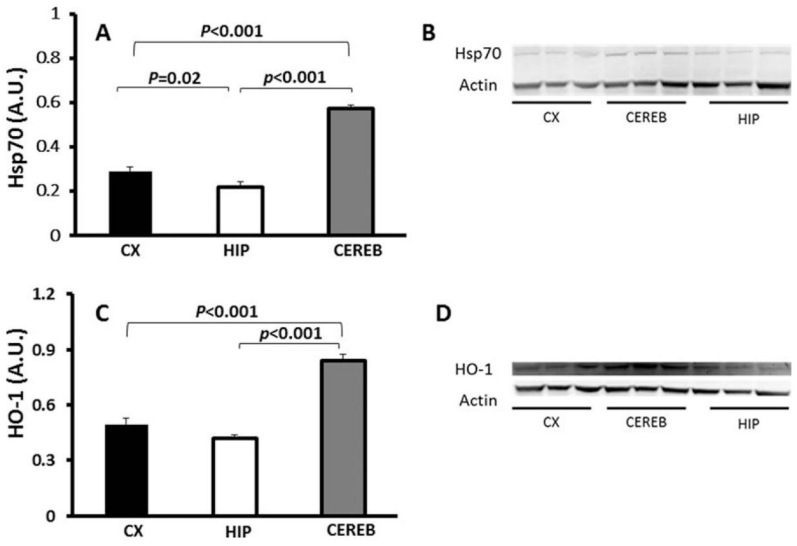

Fig. 7.

Regional distribution of Hsp70 and HO-1. **A:** Average Hsp70 levels were significantly different among NMR brain regions (ANOVA F = 94.7, $P < 0.001$) as measured by immunoblot. Levels of Hsp70 were the lowest in hippocampus compared with both cortex ($P = 0.02$) and cerebellum ($P < 0.001$). **B:** Representative image of immunoblot stained for Hsp70. **C:** Average levels of HO-1 were also significantly different among brain regions (ANOVA F = 52.32, $P < 0.001$). The cerebellum had the highest levels compared with both hippocampus ($P < 0.001$) and cortex ($P < 0.001$). **D:** Representative image of immunoblot stained for HO-1. Data are mean ± SEM (n = 6).